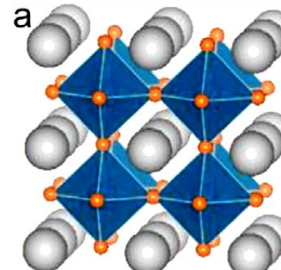
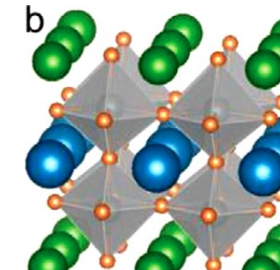
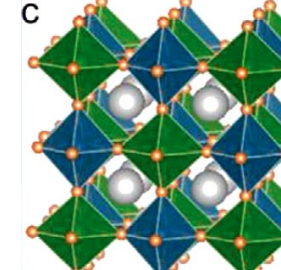
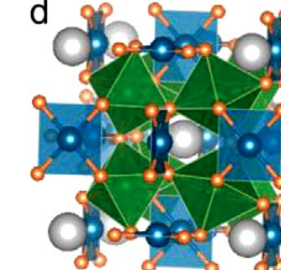


Table S1. Comparison of single perovskite oxides, double perovskite oxides, and quadruple perovskite oxides from aspects of their crystal structures and physical properties.

	Single perovskite oxides	Double perovskite oxides (DPOs)		A- and B-site-ordered quadruple perovskite oxides
		A-site ordered DPOs	B-site ordered DPOs	
General formula	ABO_3	$\text{A}'\text{A}''\text{B}_2\text{O}_6$	$\text{A}_2\text{B}'\text{B}''\text{O}_6$	$\text{AA}'_3\text{B}'_2\text{B}''_2\text{O}_{12}$
Crystal structure	 Cubic, space group $Pm\bar{3}m$;	 Cubic, space group $R\bar{3}2$ or $Imm2$;	 Cubic, space group $Fm\bar{3}m$ or Monoclinic, space group $P2_1/n$	 Cubic, space group $Pn\bar{3}$
Magnetic interactions	B-B interaction (or B-O-B interaction via oxygen ions)	$\text{A}''\text{-B}$, $\text{A}''\text{- A}''$, B-B interactions	$\text{B}'\text{-B}'$, $\text{B}''\text{-B}''$, $\text{B}'\text{-B}''$ interactions	$\text{A}'\text{-A}'$, $\text{A}'\text{-B}'$, $\text{A}'\text{-B}''$, $\text{B}'\text{-B}''$, $\text{B}'\text{-B}'$ and $\text{B}''\text{-B}''$ interactions
Structural flexibility	In ABO_3 simple perovskite (orthorhombic, $Pnma$) with AO_8 and BO_6 coordination environment, the B-O-B tilt angles are within the range of 140–180°. Random arrangements of the cation distribute along 3D directions.	$\text{A}'\text{A}''\text{B}_2\text{O}_6$ double perovskite oxides have a lamella structure with a stacking sequence of $-\text{A}'\text{O}-\text{BO}_2-\text{A}''\text{O}-\text{BO}_2-$, and A' and A'' cations are arranged alternatively along the [001] crystallographic axis.	Distorted $\text{A}_2\text{B}'\text{B}''\text{O}_6$ double perovskite (monoclinic, $P2_1/n$) exhibits rock-salt ordering B' and B'' and eight-coordination AO_8 . B' and B'' cations are arranged alternatively along the [111] crystallographic axis.	$\text{AA}'_3\text{B}'_2\text{B}''_2\text{O}_{12}$ quadruple perovskite oxides with 1:3 ordering A-site arrangement, have icosahedral AO_{12} , square planar $\text{A}'\text{O}_4$, and $\text{B}'\text{O}_6$ and $\text{B}''\text{O}_6$ octahedra. This special perovskite family is formed in the $a^+a^+a^+$ tilt system with very large B-O-B tilt angles of 140–145°.
Compositional flexibility	There are 32/54 kinds of elements that have been found at the A/B site with diverse oxidation states ranging from 1+ to 7+ and a wide range of ionic radii of 0.76 Å (Li^+)–1.52 Å	Layered ordering of an $\text{A}'\text{A}''\text{B}_2\text{O}_6$ perovskite results in $P4/mmm$ space group symmetry. This arrangement leads to three chemically distinct environments	The structure has extremely large tolerance to different elemental combinations of (B' and B''). To maintain the charge balance, $\text{A}_2\text{B}'\text{B}''\text{O}_6$ must satisfy	$\text{AA}'_3\text{B}'_2\text{B}''_2\text{O}_{12}$ quadruple perovskite oxides combine the advantages of A- and B-site-ordered quadruple perovskite oxides. Unlike the A-site in the basic ABO_3

	(K ⁺) for A and 0.45 Å (Be ²⁺)–1.52 Å (K ⁺) for B, exhibiting large flexibility of compositions that can form the crystal structure of perovskites. In theory, there are 2346 kinds of ABO ₃ and at least 265 of them have been experimentally synthesized [1].	for the anions a structural instability when the sizes and/or bonding strengths of the A' and A'' cations are significantly different. Thus, layered ordering of A-site cations only partially alleviates the lattice strains associated with an A'/A'' size mismatch. From an electrostatic point of view rock salt ordering must also be preferable for A-site cations, yet long-range rock salt ordering of A-site cations is very rare [2].	the following equation of $2Q_A + Q_{B'} + Q_{B''} = 12$ [1]. There are thousands of the A ₂ B'B''O ₆ DPOs reported in the literature which were synthesized under ambient pressure [3]. Many new DPs were also synthesized at high-pressure.	perovskites, which is usually occupied by alkali-metal, alkaline-earth or rare-earth cations, the A'-site in AA' ₃ B' ₂ B'' ₂ O ₁₂ can accommodate transition metal ions. The introduction of A'-A', A'-B' and A'-B'' magnetic interactions in addition to B'-B'', B'-B' and B''-B'' couplings results in a variety of intriguing properties [4]. A large number of consistent elements can be introduced into A, A', B' and B''-sites by high pressure synthesis method.
Modulation of physical properties	Physical properties of the ABO ₃ simple perovskite are controlled by partial or complete substitution of the A-/B-site cations. The B-B interaction is dominantly responsible for the physical properties.	Physical properties of the A'A''B ₂ O ₆ double perovskites are not only controlled by the B-B interaction (mainly responsible for the properties of simple perovskites) but also the A''-A'' and A''-B interactions.	Instead of the B-B interaction in a simple ABO ₃ perovskite, B'-B'' interaction mainly contributes to the physical properties of A ₂ B'B''O ₆ with a rock-salt ordered structure at B-site.	Physical properties of the AA' ₃ B' ₂ B'' ₂ O ₁₂ quadruple perovskite oxides are controlled by the multiple interactions between transition metal ions, i.e., A'-A', A'-B', A'-B'', B'-B'', B'-B' and B''-B'' interactions, which are complete each other.
Magnetic transition temperature (<i>T_C</i>)	Simple ABO ₃ perovskite compounds, La _{0.67} Ba _{0.33} Mn _{1-x} Cr _x O ₃ (0 ≤ x ≤ 0.15), are reported to have <i>T_C</i> values ranging from 275 K to 345 K [5]. The decrease of <i>T_C</i> is mainly interpreted by the decrease of the B-O-B bond angle and the increase of the B-O bond length as the Cr	A ₂ B'B''O ₆ DPOs with a 3d transition metal ion at the B'-site and a 4d or 5d transition metal ion at the B''-site, are reported to exhibit magnetic transition temperatures ranging from ~ 200 K to ~ 800 K [6]. For example, Sr-based Sr ₂ B'B''O ₆ DPOs such as Sr ₂ FeReO ₆ (<i>T_C</i> = 432 K) [7], Sr ₂ FeWO ₆ (<i>T_C</i> ≈ 450 K) [8], Sr ₂ FeMoO ₆ (<i>T_C</i> ≈ 420 K) [9], Sr ₂ CrMoO ₆ (<i>T_C</i> = 450 K) [10], Sr ₂ CrReO ₆ (<i>T_C</i> = 635 K) [1q], Sr ₂ CrWO ₆ (<i>T_C</i> = 390 K) [12], and Sr ₂ CrOsO ₆ (<i>T_C</i> = 725 K) [13] are reported.	In the AA' ₃ B' ₂ B'' ₂ O ₁₂ quadruple perovskite oxides with the <i>Pn</i> ̄ ³ space group, the A'-A', A'-B/B'-B/B' interactions can further enhance and/or tune the physical properties. For example, the <i>T_C</i> value of quadruple perovskite oxide LaCu ₃ Fe ₂ Re ₂ O ₁₂ was	

	content increases.		reported to be 710 K due to the strong Cu ²⁺ (↑) Fe ³⁺ (↑) Re ^{4.5+} (↓) spin interactions [14].
Magnetization ($\mu_B/\text{f.u.}$)	Simple ABO ₃ perovskite compounds, La _{0.67} Ba _{0.33} Mn _{1-x} Cr _x O ₃ (0 ≤ x ≤ 0.15), are reported to have magnetization values ranging from 2.73 to 3.49 $\mu_B/\text{f.u.}$ [5].	For A ₂ B'B''O ₆ DPOs, a fully ordered state in an ideal state will result in a maximum saturation magnetization (M_S). For example, in theory, M_S is 2.0 $\mu_B/\text{f.u.}$ in fully ordered Bi ₂ FeCrO ₆ and Bi ₂ NiMnO ₆ thin films [15,16], and even higher in fully ordered La ₂ CoMnO ₆ thin films, M_S = 6.0 $\mu_B/\text{f.u.}$ [17,18]. This value can be used to estimate the degree of “magnetic” ordering.	Quadruple perovskite oxide LaCu ₃ Fe ₂ Re ₂ O ₁₂ has a large saturation magnetization (M_S) of 8.7 $\mu_B/\text{f.u.}$, which is considerably enhanced compared with those observed in A ₂ FeReO ₆ (A = Ca, Sr and Ba) DPOs [19-21].

1. W. J. Yin, B. C. Weng, J. Ge, Q. D. Sun, Z. Z. Li and Y. F. Yan, *Energy Environ. Sci.*, 2019, **12**, 442-462.
2. M. C. Knapp and P. M. Woodward, *J. Solid State Chem.*, 2006, **179**, 1076–1085.
3. S. Vasala and M. Karppinen, *Prog. Solid State Chem.*, 2015, **43**, 1–36.
4. Y. Shimakawa and M. Mizumaki, *J. Phys.: Condens. Matter*, 2014, **26**, 473203.
5. M. Oumezzine, O. Pena, Sami Kallel, T. Guizouarn and M. Oumezzine, *J. Alloys Compd.*, 2012, **533**, 33-40.
6. T. K. Mandal, C. Felser, M. Greenblatt and J. Kübler, *Phys. Rev. B*, 2008, **78**, 134431.
7. K. Leng, Q. K. Tang, Z. W. Wu, K. Yi and X. H. Zhu, *J. Am. Ceram. Soc.*, 2022, **105**, 4097–4107.
8. F. Bardelli, C. Meneghini, S. Mobilio, S. Ray and D.D. Sarma, *J. Phys.: Condens. Matter*, 2009, **21**, 195502.
9. K.-I. Kobayashi, T. Kimura, H. Sawada, K. Terakura and Y. Tokura, *Nature*, 1998, **395**, 677–680.
10. Z. C. Wang, L. Chen, S. S. Li, J. S. Ying, F. Tang, G. Y. Gao, Y. Fang and W. Zhao, *NPJ Quantum Mater.*, 2021, **53**, 1–8.
11. L. Fuoco, D. Rodriguez, P. Tim, P.A.Maggard, *Chem. Mater.* 23 (2011) 5409–5414.
12. J. B. Philipp, P. Majewski, L. Alff, A. Erb, R. Gross, T. Graf, M. S. Brandt, J. Simon, T. Walther, W. Mader, D. Topwal and D. D. Sarma, *Phys. Rev. B*, 2003, **68**, 144431.
13. Y. Krockenberger, K. Mogare, M. Reehuis, M. Tovar, M. Jansen, G. Vaitheeswaran, V. Kanchana, F. Bultmark, A. Delin, F. Wilhelm, A. Rogalev, A. Winkler and L. Alff, *Phys. Rev. B*, 2007, **75**, 020404(R).

14. Z. Liu, S. Zhang, X. Wang, X. Ye, S. Qin, X. Shen, D. Lu, J. Dai, Y. Cao, K. Chen, F. Radu, W. -B. Wu, C. T. Chen, S. Francoual, J. R. L. Mardegan, O. Leupold, L. H. Tjeng, Z. Hu, Y. Yang and Y. Long, *Adv. Mater.*, 2022, **34**, 2200626.
15. P. Baettig and N. A. Spaldin, *Appl. Phys. Lett.*, 2005, **86**, 012505.
16. O. Dieguez and J. Iniguez, *Phys. Rev. B*, 2017, **95**, 085129.
17. H. Z. Guo, A. Gupta, T. G. Calvarese and M. A. Subramanian, *Appl. Phys. Lett.*, 2006, **89**, 262503.
18. M. P. Singh, S. Charpentier, K. D. Truong and P. Fournier, *Appl. Phys. Lett.*, 2007, **90**, 211915.
19. D. Serrate, J. M. De Teresa and M. R. Ibarra, *J. Phys.: Condens. Matter*, 2007, **19**, 023201.
20. W. Prellier, V. Smolyaninova, A. Biswas, C. Galley, R. L. Greene, K. Ramesha and J. Gopalakrishnan, *J. Phys.: Condens. Matter*, 2000, **12**, 965-973.
21. J. Gopalakrishnan, A. Chattopadhyay, S. B. Ogale, T. Venkatesan, R. L. Greene, A. J. Millis, K. Ramesha, B. Hannoyer and G. Marest, *Phys. Rev. B*, 2000, **62**, 9538-9542.

Table S2. Summaries of quadruple perovskite oxides synthesized by different methods and their crystal structures and physical properties

Synthesized methods	Quadruple perovskite oxides	Crystal structures	Physical properties	Reference
Solid-state reaction (SSR) method	A-site ordered perovskite $\text{AA}'_3\text{B}_4\text{O}_{12}$			
	$\text{CaCu}_3\text{Ti}_4\text{O}_{12}$	Cubic, $I\bar{m}\bar{3}$	AFM, $T_N \approx 25$ K, $M_s = 0.56 \mu_B/\text{f.u.}$, $\varepsilon_r \sim 10286$, $\tan \delta \sim 0.067$	1-3
	$\text{ACu}_3\text{Ru}_4\text{O}_{12}$ (A = Ca, La, and Nd)			
	$\text{CaCu}_3\text{Ru}_4\text{O}_{12}$	Cubic, $I\bar{m}\bar{3}$	PM, $M_s = 0.32 \mu_B/\text{f.u.}$, $\rho_{0(1.5\text{ K})} = 0.110 \text{ m}\Omega\cdot\text{cm}$	4,5
	$\text{LaCu}_3\text{Ru}_4\text{O}_{12}$		$\rho_{0(1.5\text{ K})} = 0.313 \text{ m}\Omega\cdot\text{cm}$, $\rho_{300\text{ K}} = 1.28 \text{ m}\Omega\cdot\text{cm}$, $\Theta = 390$ K	6,7
	$\text{NdCu}_3\text{Ru}_4\text{O}_{12}$		$\rho_{0(1.5\text{ K})} = 0.474 \text{ m}\Omega\cdot\text{cm}$, $\Theta = 390$ K	6
	A-site columnar-ordered perovskite $\text{A}_2\text{A}'\text{A}''\text{B}_4\text{O}_{12}$			
	$\text{CaMnTi}_2\text{O}_6$ (HT-HP)	Tetragonal, $P4_2mc$	$T_c = 630$ K, $P = 24 \mu\text{C}/\text{cm}^2$, $P_r = 3.5 \mu\text{C}/\text{cm}^2$, $E_c = 53$ kV/cm	8
	$\text{CaFeTi}_2\text{O}_6$ (HT-HP)	Tetragonal, $P4_2/nmc$	-	9
	MnLaMnSbO_6 MnPrMnSbO_6 MnNdMnSbO_6 MnSmMnSbO_6 (HT-HP)	Tetragonal, $P4_2/n$	$T_c = 48$ K, $\mu_{\text{th}} = 8.37 \mu_B/\text{f.u.}$ $T_c = 89$ K, $T_{N2} = 75$ K, $\mu_{\text{th}} = 9.12 \mu_B/\text{f.u.}$ $T_c = 76$ K, $T_{N2} = 42$ K, $\mu_{\text{th}} = 9.14 \mu_B/\text{f.u.}$, $\mu_{\text{exp}} = 8.9 \mu_B/\text{f.u.}$ $T_c = 48$ K, $T_{N2} = 39$ K, $\mu_{\text{th}} = 8.5 \mu_B/\text{f.u.}$, $\mu_{\text{exp}} = 8.3 \mu_B/\text{f.u.}$	10
	SmMnGaTiO_6 GdMnGaTiO_6 (HT-HP)		$\mu_{\text{eff}} = 6.21 \mu_B/\text{f.u.}$, $M_s = 2.5 \mu_B/\text{f.u.}$, $C = 4.82 \text{ emu K}$, $T_N = 3$ K $\mu_{\text{eff}} = 9.75 \mu_B/\text{f.u.}$, $M_s = 11 \mu_B/\text{f.u.}$, $C = 11.88 \text{ emu K}$, $T_N = 3$ K	
Solid-state reaction (SSR) method	RMnMn_2O_6 (R=Gd-Tm and Y) (HTHP) $\text{Tm}_{0.88}\text{Mn}_3\text{O}_{5.82}$ $\text{Er}_{0.88}\text{Mn}_3\text{O}_{5.82}$ $\text{Ho}_{0.9}\text{Mn}_3\text{O}_{5.85}$ $\text{Y}_{0.9}\text{Mn}_3\text{O}_{5.85}$ DyMn_3O_6 $\text{GdMn}_{2.833}\text{O}_{5.75}$	Orthorhombic, $Pmmn$	$\mu_{\text{eff}} = 10.608 \mu_B/\text{f.u.}$, $M_s = 6.4 \mu_B/\text{f.u.}$, $T_{N1} = 75$ K, $T_{N2} = 20$ K $\mu_{\text{eff}} = 12.318 \mu_B/\text{f.u.}$, $M_s = 6.97 \mu_B/\text{f.u.}$, $T_{N1} = 68$ K, $T_{N2} = 21$ K $\mu_{\text{eff}} = 12.917 \mu_B/\text{f.u.}$, $M_s = 6.89 \mu_B/\text{f.u.}$, $T_{N1a} = 69$ K, $T_{N1b} = 65$ K $\mu_{\text{eff}} = 8.027 \mu_B/\text{f.u.}$, $M_s = 3.05 \mu_B/\text{f.u.}$, $T_{N1a} = 69$ K, $T_{N1b} = 65$ K $\mu_{\text{eff}} = 13.444 \mu_B/\text{f.u.}$, $M_s = 7.18 \mu_B/\text{f.u.}$, $T_{N1} = 58$ K, $T_{N2} = 46$ K $\mu_{\text{eff}} = 11.095 \mu_B/\text{f.u.}$, $M_s = 6.39 \mu_B/\text{f.u.}$, $T_N = 87$ K	12

	CaMnMnReO ₆ (HT-HP) Ca(Mn _{0.5} Cu _{0.5})FeReO ₆	Tetragonal, <i>P4₂/n</i>	$T_{N1}=100\text{ K}$, $T_{N2}=120\text{ K}$, $M_s=3.4\text{ }\mu_B/\text{f.u.}$ $T_{N1}=160\text{ K}$, $T_{N2}=560\text{ K}$, $M_s=4.8\text{ }\mu_B/\text{f.u.}$	13
A- and B-site multiply ordered perovskite AA'₃B₂B'₂O₁₂				
	LaCu ₃ Fe ₂ TiSbO ₁₂	Cubic, <i>I</i> ⁻ ₃	AFM, $T_{N1}=60\text{ K}$, $T_{N2}=160\text{ K}$, $M_s=1.2\text{ }\mu_B/\text{f.u.}$	14
Hexagonal quadruple perovskite oxides				
	Ba ₄ BiIr ₃ O ₁₂	Hexagonal, <i>C2/m</i>	$T_N=215\text{ K}$, $\mu_{\text{eff}}=0.22\text{ }\mu_B/\text{Ir.}$	15
	Ba ₄ EuRu ₃ O ₁₂ Ba ₄ EuIr ₃ O ₁₂	Hexagonal, <i>C2/m</i>	AFM, $T_N=4\text{ K}$, $\mu_{\text{eff}}=1.18\text{ }\mu_B/\text{f.u.}$, $E_a=0.18\text{ eV}$ PM, $E_a=0.22\text{ eV}$, $\Theta_p = -0.773\text{K}$	16
	Ba ₄ LuRu ₃ O ₁₂ Ba ₄ NdRu ₃ O ₁₂	Hexagonal, <i>R-3m</i> Hexagonal, <i>C2/m</i>	AFM, $\mu_{\text{eff}}=2.86\text{ }\mu_B/\text{f.u.}$, $T_N=8\text{ K}$ FiM, $\mu_{\text{eff}}=4.7\text{ }\mu_B/\text{f.u.}$, $T_N=11.5\text{ K}$	17
	Ba ₄ CuNb ₃ O ₁₂	Hexagonal, <i>P6₃/mmc</i>	-	18
A-site ordered perovskite AA'₃B₄O₁₂				
Sol-gel method	CaCu ₂ MnTi ₃ MnO ₁₂	Cubic, <i>I</i> ⁻ ₃	AFM, $\mu_{\text{eff}}=3.85\text{ }\mu_B/\text{f.u.}$, $\varepsilon_r \sim 2040$	19
	CdCu ₃ Fe ₄ O ₁₂	Cubic, <i>I</i> ⁻ ₃	FM/AFM, $T_c=190\text{ K}$, $T_N=170\text{ K}$, $M_s=1.6\text{ }\mu_B/\text{f.u.}$	20
	LaCu ₃ Mn ₃ TiO ₁₂ LaCu ₃ Mn _{3.5} Ti _{0.5} O ₁₂ LaCu ₂ Mn ₄ TiO ₁₂	Cubic, <i>I</i> ⁻ ₃	AFM, $T_c=230\text{ K}$, $M_s=8.6\text{ }\mu_B/\text{f.u.}$, $M_{\text{cal}}=7\text{ }\mu_B/\text{f.u.}$ AFM, $T_c=235\text{ K}$, $M_s=10.4\text{ }\mu_B/\text{f.u.}$, $M_{\text{cal}}=8.5\text{ }\mu_B/\text{f.u.}$ AFM, $T_c=225\text{ K}$, $M_s=10.82\text{ }\mu_B/\text{f.u.}$, $M_{\text{cal}}=9\text{ }\mu_B/\text{f.u.}$	21
	A- and B-site multiply ordered perovskite AA'₃B₂B'₂O₁₂			
	CaCu ₃ Fe ₂ Sb ₂ O ₁₂	Cubic, <i>Pn</i> ⁻ ₃	AFM, $T_N=160\text{ K}$, $M_s=5.35\text{ }\mu_B/\text{f.u.}$, $\rho > 10^7\text{ }\Omega$	22
A-site columnar-ordered perovskite A₂A'A''B₄O₁₂				
	Y ₂ CuMnMn ₄ O ₁₂	<i>Pmmn</i>	PM, $T_N=175\text{K}/159\text{K}$	26

High temperature and high pressure	$\text{Ho}_2\text{MnGaMn}_4\text{O}_{12}$	$P4_2/nmc$	$\mu_{\text{eff}}=18.428 \mu_{\text{B/f.u.}}$, $\Theta_p=-21.5(3) \text{ K}$	27
	$\text{Dy}_2\text{CuMnMn}_4\text{O}_{12}$	$Pmmn$	$T_{\text{N}1}=160 \text{ K}$, $T_{\text{N}2}=125 \text{ K}$, $T_{\text{N}3}=21 \text{ K}$	27
	$\text{Y}_2\text{CuMnMn}_4\text{O}_{12}$	$Pmmn$	PM, $T_{\text{N}}=175\text{K}/159\text{K}$	26
	A- and B-site multiply ordered perovskite $\text{AA}'_3\text{B}_2\text{B}'_2\text{O}_{12}$			
	$\text{CaCu}_3\text{Co}_2\text{Re}_2\text{O}_{12}$	Cubic, $Pn\bar{3}$	FiM/FM, $\mu_{\text{eff}}=10.09 \mu_{\text{B/f.u.}}$, $M_s=4 \mu_{\text{B/f.u.}}$, $T_c=20 \text{ K}$, $T_{\text{N}}=28 \text{ K}$, $C=12.1 \text{ emu K Oe}^{-1} \text{ mol}^{-1}$	28
	$\text{CaCu}_3\text{Fe}_2\text{Re}_2\text{O}_{12}$	Cubic, $Pn\bar{3}$	FiM, $M_s=8.7 \mu_{\text{B/f.u.}}$, $T_c=560 \text{ K}$, $T_{\text{N}}=28 \text{ K}$, $\rho=10 \text{ m}\Omega\cdot\text{cm}$	29
	$\text{LaMn}_3\text{Ni}_2\text{Mn}_2\text{O}_{12}$	Cubic, $Pn\bar{3}$	FM, $M_s=6.6 \mu_{\text{B/f.u.}}$, $T_c=34 \text{ K}$, $T_{\text{N}}=46 \text{ K}$	30
	$\text{NaCu}_3\text{Fe}_2\text{Os}_2\text{O}_{12}$	Cubic, $Pn\bar{3}$	FiM, $T_c=380 \text{ K}$, $M_s=5.5 \mu_{\text{B/f.u.}}$	31

FM: Ferromagnetic; AFM: Antiferromagnetic; PM: Paramagnetic; FiM Ferrimagnetic, T_{N} : Neel temperature; T_c : Curie temperatures; ρ : Electrical resistivity; ρ_0 : Residual resistivity; Θ : Einstein temperature; E_c : Coercive field; P : Spontaneous Polarization; μ_{eff} : Effective moment; μ_{th} : Theoretical moment; μ_{exp} : Experimental moments; C : Curie constants; E_a : Activation energies; Θ_p : Curie-Weiss temperature; M_{cal} : Calculated magnetization; M_s : Saturation magnetization; ε_r : Dielectric constant; $\tan \delta$: Dielectric loss.

Reference

1. P. Y. Raval, P. R. Pansara, A. R. Makadiya, N. H. Vasoya, S. N. Dolia and K. B. Modi, *Ceram. Int.*, 2018, **44**, 17667-17674.
2. M. A. Subramanian, D. Li, N. Duan, B. A. Reisner and A. W. Sleight, *J. Solid State Chem.*, 2000, **151**, 323-325.
3. J. K. Bidika, A. Chauhan and B. R. K. Nanda, *Phys. Rev. B*, 2022, **106**, 115152.
4. T. Kida, R. Kammuri, M. Hagiwara, S. Yoshii, W. Kobayashi, M. Iwakawa and I. Terasaki, *Phys. Rev. B*, 2012, **85**, 195122.
5. A. Krimmel, A. Günther, W. Kraetschmer, H. Dekinger, N. Büttgen, A. Loidl, S. G. Ebbinghaus, E. W. Scheidt and W. Scherer, *Phys. Rev. B*, 2008, **78**, 165126.
6. A. Günther, S. Riegg, W. Kraetschmer, S. Wehrmeister, N. Büttgen, E. W. Scheidt, H. A. K. von Nidda, M. V. Eremin, E. A. Arkhipova, R. M. Eremina, A. Krimmel, H. Mutka and A. Loidl, *Phys. Rev. B*, 2020, **102**, 235136.
7. S. Hébert, R. Daou and A. Maignan, *Phys. Rev. B*, 2015, **91**, 045106.
8. A. Aimi, D. Mori, K.-i. Hiraki, T. Takahashi, Y. J. Shan, Y. Shirako, J. Zhou and Y. Inaguma, *Chem. Mater.*, 2014, **26**, 2601-2608.
9. K. Leinenweber and J. Parise, *J. Solid State Chem.*, 1995, **114**, 277-281.
10. E. Solana-Madruga, A. M. Arevalo-Lopez, A. J. Dos Santos-Garcia, E. Urones-Garrote, D. Avila-Brande, R. Saez-Puche and J. P. Attfield, *Angew. Chem., Int. Ed.*, 2016, **55**,

9340-9344.

11. G. Shimura, K. Niwa, Y. Shirako and M. Hasegawa, *Eur. J. Inorg. Chem.*, 2017, **2017**, 835-839.
12. L. Zhang, Y. Matsushita, K. Yamaura and A. A. Belik, *Inorg. Chem.*, 2017, **56**, 5210-5218.
13. G. M. McNally, Á. M. Arévalo-López, P. Kearins, F. Orlandi, P. Manuel and J. P. Attfield, *Chem. Mater.*, 2017, **29**, 8870-8874.
14. L. Kumar, J. Datta, S. Sen, P. P. Ray and T. K. Mandal, *J. Solid State Chem.*, 2021, 302.
15. W. Müller, M. T. Dunstan, Z. Huang, Z. Mohamed, B. J. Kennedy, M. Avdeev and C. D. Ling, *Inorg. Chem.*, 2013, **52**, 12461-12467.
16. Y. Shimoda, Y. Doi, M. Wakshima and Y. Hinatsu, *Inorg. Chem.*, 2009, **48**, 9952-9957.
17. Y. Shimoda, Y. Doi, M. Wakshima and Y. Hinatsu, *J. Solid State Chem.*, 2010, **183**, 1962-1969.
18. N. Kumada, W. Zhang, Q. Dong, T. Mochizuki, Y. Yonesaki, T. Takei and N. Kinomura, *Powder Diffr.*, 2012, **26**, 244-247.
19. K. Pal, A. Dey, P. P. Ray, N. E. Mordinova, O. I. Lebedev, T. K. Mandal, M. M. Seikh and A. Gayen, *ChemistrySelect*, 2018, **3**, 1076-1087.
20. I. Yamada, A. Takamatsu, N. Hayashi and H. Ikeno, *Inorg. Chem.*, 2017, **56**, 9303-9310.
21. A. Haque, R. Das, M. Vasundhara, D. Ghosh, A. Gayen, P. Mahata, A. K. Kundu and M. M. Seikh, *J. Alloys Compd.*, 2021, **875**, 159984.
22. S. A. Larregola, J. Zhou, J. A. Alonso, V. Pomjakushin and J. B. Goodenough, *Inorg. Chem.*, 2014, **53**, 4281-4283.
23. Y. Okazaki, Y. Kato, Y. Kizawa, S. Oda, K. Uemura, T. Nishio, F. Fujii, S. Fujinari, M. Kinoshita, T. Odake, H. Togano, T. Kamegawa, S. Kawaguchi, H. Yamamoto, H. Ikeno, S. Yagi, K. Wada, K. H. Ahn, A. Hariki and I. Yamada, *Inorg. Chem.*, 2021, **60**, 7023-7030.
24. J. Guo, S. Y. Wang, W. M. Li, D. B. Lu, X. B. Ye, Z. H. Liu, S. J. Qin, X. Wang, Z. W. Hu, H. J. Lin, C. T. Chen, J. G. Wan, Q. F. Zhang and Y. W. Long, *Phys. Rev. B*, 2022, **105**, 054409.
25. H. Etani, I. Yamada, K. Ohgushi, N. Hayashi, Y. Kusano, M. Mizumaki, J. Kim, N. Tsuji, R. Takahashi, N. Nishiyama, T. Inoue, T. Irifune and M. Takano, *J. Am. Chem. Soc.*, 2013, **135**, 6100-6106.
26. A. M. Vibhakar, D. D. Khalyavin, P. Manuel, J. Liu, A. A. Belik and R. D. Johnson, *Phys. Rev. Lett.*, 2020, **124**, 127201.
27. A. A. Belik, D. D. Khalyavin, L. Zhang, Y. Matsushita, Y. Katsuya, M. Tanaka, R. D. Johnson and K. Yamaura, *Chemphyschem*, 2018, **19**, 2449-2452.
28. Z. H. Liu, X. Wang, X. B. Ye, X. D. Shen, Y. C. Bian, W. Ding, S. Agrestini, S. C. Liao, H. J. Lin, C. T. Chen, S. C. Weng, K. Chen, P. Ohresser, L. Nataf, F. Baudelet, Z. G. Sheng, S. Francoual, J. R. L. Mardegan, O. Leupold, Z. F. Li, X. K. Xi, W. H. Wang, L. H. Tjeng, Z. W. Hu and Y. W. Long, *Phys. Rev. B*, 2021, **103**, 014414.
29. W. T. Chen, M. Mizumaki, H. Seki, M. S. Senn, T. Saito, D. Kan, J. P. Attfield and Y. Shimakawa, *Nat. Commun.*, 2014, **5**, 3909.
30. Y.-Y. Yin, M. Liu, J.-H. Dai, X. Wang, L. Zhou, H. Cao, C. dela Cruz, C.-T. Chen, Y. Xu, X. Shen, R. Yu, J. A. Alonso, A. Muñoz, Y.-F. Yang, C. Jin, Z. Hu and Y. Long, *Chem. Mater.*, 2016, **28**, 8988-8996.
31. X. Wang, M. Liu, X. Shen, Z. Liu, Z. Hu, K. Chen, P. Ohresser, L. Nataf, F. Baudelet, H. J. Lin, C. T. Chen, Y. L. Soo, Y. F. Yang, C. Jin and Y. Long, *Inorg. Chem.*, 2019, **58**, 320-326.